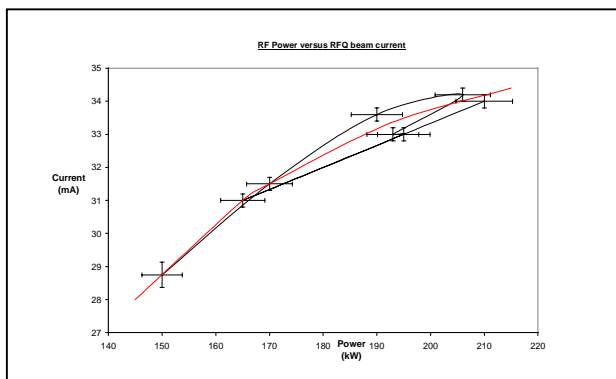


# MEASUREMENTS OF BEAM ENERGY USING THE GAS SCATTERING SYSTEM IN THE ISIS RFQ TEST STAND

J P Duke, D J S Findlay, S Hughes, P Knight, G R Murdoch, CLRC, RAL, Chilton, Didcot

## Abstract

The new RFQ accelerator for the ISIS Spallation Neutron Source at the Rutherford Appleton Laboratory (RAL) is designed to accelerate  $H^-$  particles from 35 keV to 665 keV. Beams have already been successfully accelerated through the RFQ, and now investigations are continuing into the detailed properties of the accelerated beam using the RFQ Test Stand at RAL. A novel system has been set up in which the beam of accelerated particles is attenuated in cascaded multiple scattering cells filled with xenon gas and the energies of the particles are measured using a semiconductor particle detector. Measurements and results are reported.



## 1 SUMMARY OF APPARATUS

The purpose of the apparatus is to confirm the mean energy and energy spread of the nominal 665 keV beam from the ISIS RFQ. This RFQ, after comprehensive testing, is intended to replace the existing Cockcroft-Walton pre-injector on the ISIS spallation neutron source at the Rutherford Appleton Laboratory (RAL). The RFQ is performing well, and as can be seen from Fig. 2 below, is able to transport greater than its design current of 30mA at well below its designed RF power of about 200kW.

A more detailed description of the design process for the apparatus used can be found at [1]. Its basis is a set of two cascaded assemblies each consisting of a 130mm long gas scattering cell, a 0.5m drift length and three small (~0.2mm diameter) apertures, which together reduce the peak intensity of the beam current sufficiently to allow a semiconductor charged particle detector [2] to be used to detect individual  $H^-$  ions and measure their energies. Xenon gas (at low pressure) is used to scatter the  $H^-$  beam because the higher the atomic number of the scatterer the lower is the energy loss for a given mean multiple scattering angle. The energy loss caused by the xenon is calculated for the relevant scattering thicknesses

used and is added back in as a small correction to the measured energies.

The particle detector used was an Ortec® BA-025-025-1500 silicon surface barrier detector with an active area of 25 mm<sup>2</sup> and a depletion depth of 1.5 mm, and was operated at a bias voltage of 185.9 V. Signals from the detector pass first through an EG&G Ortec® [2] Model 1421H pre-amplifier and then into a Canberra® Model 2020 spectroscopy amplifier with 1µs pulse shaping. The bipolar output from the amplifier is passed into a TRUMP PCI-8k multi-channel buffer PC card. Ortec® Maestro-32 spectrum analysis software is used to visualise and analyse the resultant spectra. Before taking a measurement the system is calibrated by fitting two adjacent gaussian curves to the 624 and 656 keV peaks of the spectrum obtained from a 2kBq Cs-137 conversion electron source, which is installed in the detector box on a movable arm. After calibration the bias voltage is never changed.

## 2 EXPERIMENTAL PROCEDURE

At the beginning of every experiment the whole gas scattering system is at high vacuum,  $\sim 1 \times 10^{-6}$  mbar. It is necessary to ensure no beam is allowed onto the detector before there is xenon gas in the gas cells because the detector would almost certainly be destroyed. So, after the vacuum valves to the gas cells have been closed, the needle valves to the gas cells are opened very slowly, until the pressure starts to rise. Then the valves are used to control the pressure rise so that the pressure reaches an equilibrium between the gas being introduced into the cell and the gas leaking out through the apertures. By carefully and slowly altering the position of the needle valves it is possible to reach and maintain a constant chosen pressure, to within about 5% at worst. Pressures must be monitored regularly throughout the experiment to maintain the chosen value and the needle valves adjusted if necessary. According to the theoretical study performed in [1], the optimum pressure for a reasonable count rate at the detector was predicted to be at about 0.02–0.03 mbar. In actual fact at this pressure the count rate was too high and produced too much pile up of particles, which resulted in ‘double’ and ‘triple’ energy peaks in the spectrum from when two or more particles arrive at the detector simultaneously. A much cleaner spectrum could be obtained with the pressure at around 0.1mbar, and most spectra were taken at about this pressure. At this pressure about one particle per beam pulse arrives at the detector, (equivalent to about 50 per second). However, although the spectrum is much cleaner, the count rate is obviously lower, so it means that it takes longer to accumulate

enough particles to get a reasonably good spectrum without too much random variation. Most spectra taken took between 30 minutes and 1 hour to accumulate. The data are saved and translated into text files for processing.

## 2.1 Data Processing

For the present purpose, the energy spectrum of the beam from the RFQ was assumed to be gaussian, with an adjustable height, mean and width. The energy lost in the xenon was obtained using polynomial interpolation amongst tabulated values of proton stopping power in xenon as a function of proton energy [3], and amounted to only  $\sim 1.8$  keV for the gas pressures used. The gaussian was then shifted down in energy by this amount. The energy straggling in the xenon was also computed, [4] but at widths of  $\sim 2 \times 10^{-2}$  keV was negligible in comparison with the typical widths of the energy spectrum. The gaussian was then convoluted with the detector resolution function, a gaussian with a FWHM of 14.1 keV obtained from the conversion electron calibration measurements. The parameters (height, mean energy and width) of the simulated original gaussian distribution were altered until a best fit with the spectrum data was obtained. Then the parameters were varied about the best fit to estimate plausible uncertainties. Good fits were obtained in most cases down to well below half height. In all cases, the wings of the measured distributions were underestimated by the fits, and for lower RF powers the lower energy “half-width” was greater than the higher energy “half-width”. This is postulated to be due to RFQ beam particles being more likely to fall out of the lowered RF bucket on the low energy side than the high energy side before they reach the end of the RFQ. One effect not yet taken into account in the results below is that of stripping of  $H^-$  ions in xenon. It has been previously calculated that at the pressures used in this experiment, almost all the  $H^-$  ions should be stripped to  $H^+$ . Therefore the two electrons will carry off some small fraction of the  $H^-$  particles’ energy. This fraction may be  $\sim 2 \cdot m_e c^2 / m_p c^2$ , i.e.  $\sim 1/918$ . Assuming a mean energy of 665 keV, this effect would add at most 0.72 keV to the energies quoted below for protons, and so is neglected for the present. Fig. 2 below shows the derived peak energies.

At lower RF powers the energy distributions become significantly asymmetric. A low energy ‘tail’ develops below about 180 kW. This can be more clearly seen by comparing Figures 3 and 4 below. Fig. 3 is the ‘symmetrical distribution’ at or near full design RF power. Fig. 4 however, is an example of the ‘asymmetrical distributions’ obtained at less than full RF power.

Fig. 5 summarises the widths of the energy spectra for various RF powers. For lower powers, the lower energy half-width becomes larger than the higher energy half-width, and this is represented by a splitting of the line of best fit into two curves, one for the high energy side and one for the low energy side.

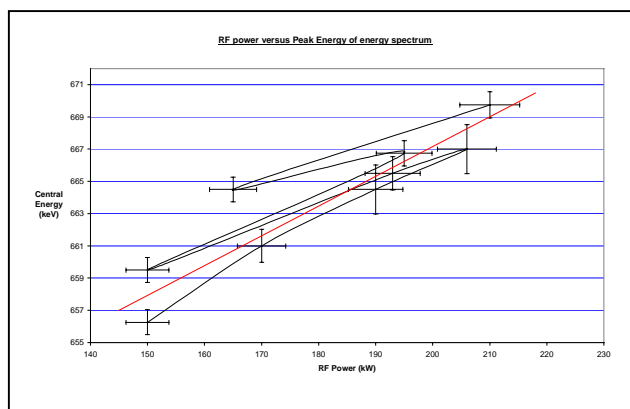


Fig.2 Peak proton energies for different RF powers

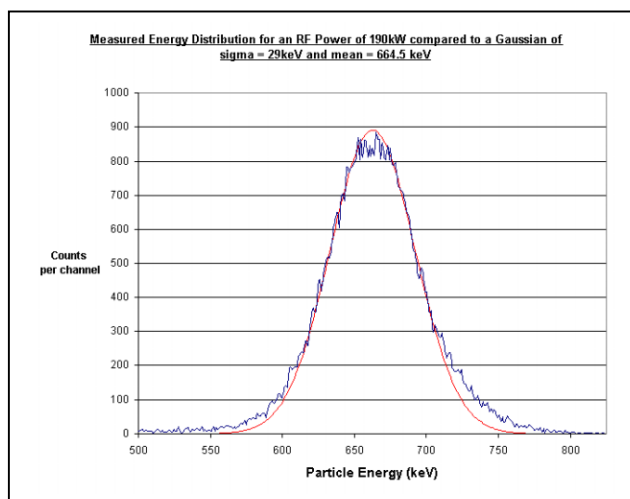


Fig. 3 ‘Symmetrical’ energy distribution at an RF power of 190kW, with ‘Gaussian Best Fit’ of standard deviation = 29keV shown in red.

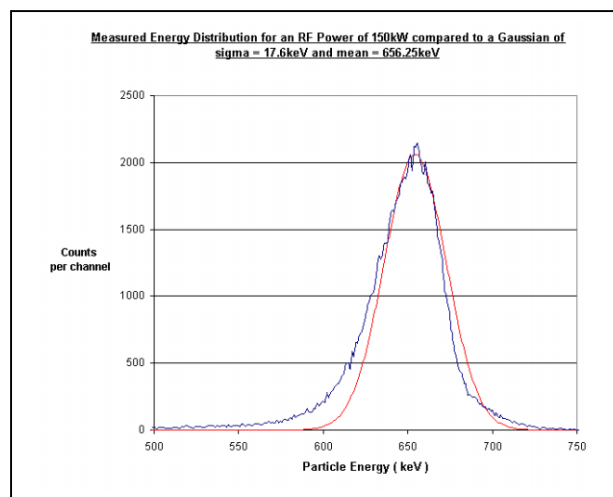


Fig.4 ‘Asymmetrical’ energy distribution at a low RF power of 150 kW compared to a gaussian (in red) with a HWHM of 20.7 keV (about half way between the widths on the low and high energy sides)

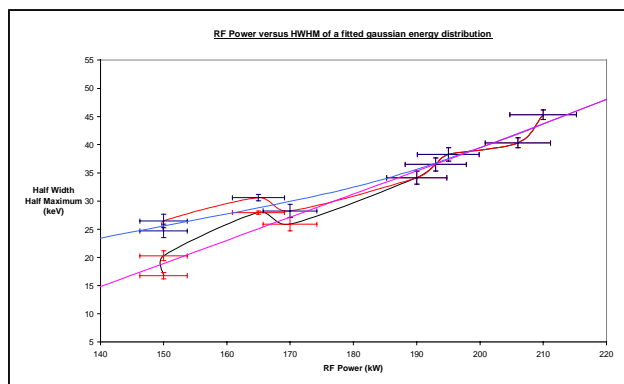


Fig. 5 RF Power versus half-widths of spectra measured from the peak energy. The light blue (higher) curve shows the HWHM of a half-gaussian fitted to the *lower* energy side of the peak, and the pink (lower) curve the HWHM of a half-gaussian fitted to the *higher* energy side of the peak. I.e. at powers < ~ 180 kW the energy distributions become asymmetric.

### 3 CONCLUSIONS

The Gas Scattering System on the ISIS RFQ Test Stand has been successfully used to measure the peak energy and energy distribution of the RFQ extracted beam for eight different RF power settings. Please note that the energy measured by this method is the ‘absolute’ energy of the beam, and not the ‘axial energy’ as measured by time of flight methods, for example. Therefore it includes the energies contained in any transverse emittances, and so should be slightly larger than the predicted extraction energy from the RFQ. However, the quoted energies do not include the effect of energy losses due to stripped electrons. The peak energy depends roughly linearly on RF power, as in the following approximate relationship:

$$E_{\text{peak}} = 0.1849 \times (\text{RF power}) + 630.2$$

The central part of the energy distributions, down to ~1/e of full height, could be fitted closely to a gaussian distribution, but below this the measured distributions were wider than the fitted distributions. The widths of the energy distributions are also basically proportional to RF power, with an approximate relationship (on the high energy side of  $E_{\text{peak}}$ ) of:

$$\text{HWHM} = 0.4150 \times (\text{RF power}) - 43.3$$

However, at powers well below the design RFQ operating power, i.e. < ~180 kW, the distributions became asymmetric, with the lower energy side becoming wider than the high energy side. Further investigations will continue in the near future, *viz.* repeating the measurements with a detector of better resolution, using longer data collection periods, including the effects of H<sup>-</sup>

stripping, and attempting to derive the original energy distributions directly from the data by deconvolution with the detector resolution function.

### 4 SUMMARY OF RESULTS

The following table summarises the results obtained in the experiments reported above. For space reasons, errors are not quoted.

RF POWER (kW)	Beam Current (mA)	$E_{\text{peak}}$ (keV)	HWHM Of gaussian beam distribution fit to spectrum data (keV)
210	34.0	669.8	45.3
206	34.2	667.0	40.3
195	33.0	666.8	38.3
193	33.0	665.5	36.5
190	33.6	664.5	34.1
170	31.5	661.0	Above $E_{\text{peak}}$ 25.9
"	"	"	Below $E_{\text{peak}}$ 28.3
165	31.0	664.5	Above $E_{\text{peak}}$ 28.0
"	"	"	Below $E_{\text{peak}}$ 30.6
150	29.0	659.5	Above $E_{\text{peak}}$ 20.3
"	"	"	Below $E_{\text{peak}}$ 26.5
150	28.5	656.3	Above $E_{\text{peak}}$ 16.8
"	"	"	Below $E_{\text{peak}}$ 24.7

Table 1. Summary of results

### 5 REFERENCES

[1] J.P.Duke, D J S Findlay, G R Murdoch-‘WPAH115’, “Design of a Gas Scattering Energy Analyser for the ISIS RFQ Accelerator Test Stand”, PAC2001, Chicago, June 2001.  
 [2] EG&G Ortec®; now part of the Ametek® Group: <http://www.ortec-online.com/>  
 [3] “Stopping-Power and Range Tables for Electrons, Protons, and Helium Ions” <http://physics.nist.gov/PhysRefData/Star/Text/contents.html>  
 [4] Bruno Rossi, “High Energy Particles”, pub. Prentice-Hall, 1952, pgs 14-15,31-32